

# An Ankle-Foot Prosthesis Emulator with Control of Plantarflexion and Inversion-Eversion Torques

Steven H. Collins<sup>†,1,2,\*</sup>, Myunghee Kim<sup>†,1</sup>, Tianjian Chen<sup>1</sup>, and Tianyao Chen<sup>3</sup>

**Abstract**—Ankle inversion-eversion compliance is an important feature of conventional prosthetic feet, and control of inversion, or roll, in robotic devices could improve balance for people with amputation. We designed a tethered ankle-foot prosthesis with two independently-actuated toes that are coordinated to provide plantarflexion and inversion-eversion torques. This configuration allows elegant, lightweight structures, with a total mass of 0.72 kg. Strain gages on the toes measure torque with less than 2.7% RMS error, while compliance in the Bowden cable tether provides series elasticity. In benchtop tests, the 90% rise time was less than 33 ms and peak torques were 180 N·m in plantarflexion and  $\pm 30$  N·m in inversion-eversion. The phase-limited closed-loop torque bandwidth was 20 Hz with a 90 N·m amplitude chirp in plantarflexion, and 24 Hz with a 20 N·m amplitude chirp in inversion-eversion. The system had low sensitivity to toe position disturbances at frequencies up to 18 Hz. Five values of constant inversion-eversion torque were applied during walking trials, in which RMS torque tracking errors were less than 3.7% in plantarflexion and less than 5.9% in inversion-eversion. This platform is therefore suitable for haptic rendering of virtual devices in experiments with humans, which may reveal strategies for improving balance or allow controlled comparisons of conventional prosthesis features. A similar morphology may be effective for autonomous devices.

## I. INTRODUCTION

Robotic prostheses can improve locomotor performance for individuals who have restricted mobility due to lower-limb amputation. During walking, these devices can restore normal ankle and knee kinematics [1], reduce metabolic rate [2], and provide direct neural control of the limb [3]. As robotic technologies improve, active prostheses are expected to enhance performance even further [4, 5].

Ankle inversion-eversion, or roll, is an important aspect of prosthesis function. Commercial prostheses typically include a passive inversion-eversion degree of freedom, either using an explicit joint [6] or a flexure [7]. This mitigates undesirable inversion moments created by uneven ground. Inversion moment has a strong effect on side-to-side motions of the body during human walking, and its pattern is altered among individuals with amputation [8]. Side-to-side motions seem to be less stable in bipedal locomotion [9, 10], particularly for amputees [11]. Difficulty controlling inversion-eversion torques in the

prosthetic ankle may partially explain reduced stability [12] and increased fear of falling and fall rates [13] among people with amputation.

Robotic prosthesis designs have begun to incorporate active control of ankle inversion-eversion. Panzenbeck and Klute [14] describe a tethered ankle prosthesis with inversion provided by a four-bar linkage and controlled by a linear actuator. The device has a mass of 2.9 kg, can produce torques of up to 34 N·m, and has a 90% rise time of 0.180 s. A plantarflexion degree of freedom is provided using a passive spring. Ficanha et al. [15] describe a prototype device intended to provide both plantarflexion and inversion-eversion control using two motors and a gimbal joint. The device has a mass of 3.0 kg. Bellman et al. [16] describe a computer model of a similar device, with estimated mass of 2.1 kg. Devices with similar peak torque but lower mass and active control of both plantarflexion and inversion-eversion would enable experimental evaluation of a larger range of assistance techniques.

The mass of prostheses with active inversion-eversion control is related to joint design. Linkages and gimbal joints often involve large parts with complex loading, resulting in increased strength and mass requirements. An alternative is suggested by the split-toe flexures in conventional passive prostheses and the actuation schemes in some powered ankle orthoses [17]. During walking, peak inversion-eversion torques are of much lower magnitude than peak plantarflexion torques [18], and the majority of the inversion impulse occurs during periods of high plantarflexion torque [19]. Coupling plantarflexion and inversion-eversion torque through the actions of two hinged toes might therefore provide sufficient inversion capacity, allowing an elegant, lightweight design.

Mechatronic performance in experimental prosthesis systems can also be improved by separating actuation hardware from worn elements. A tethered emulator approach [20–23] decouples the problems of discovering desirable prosthesis functionality from the challenges of developing fully autonomous systems. Powerful off-board motors and controllers are connected to lightweight instrumented end-effectors via flexible tethers, resulting in low worn mass and high-fidelity torque control [20, 21, 24]. Such systems can be used to haptically render virtual prostheses to human users, facilitating the discovery of novel device behaviors [25] that can then be embedded in separate autonomous designs. This approach can also be used for rapid comparison of commercial prostheses in a clinical setting [23]. To be most effective, such prosthesis emulators should have high closed-loop torque bandwidth and lightweight, strong, accurately-instrumented end-effectors.

This material is based upon work supported by the National Science Foundation under Grant No. CMMI-1300804.

<sup>†</sup>authors contributed equally to this work.

<sup>1</sup>Dept. Mechanical Engineering, Carnegie Mellon University, USA.

<sup>2</sup>Robotics Institute, Carnegie Mellon University, USA.

<sup>3</sup>Dept. Biomedical Engineering, The Catholic University of America, USA.

\*Corresponding author: S. H. Collins., 5000 Forbes Ave., Pittsburgh, PA 15213, USA. Email: stevecollins@cmu.edu

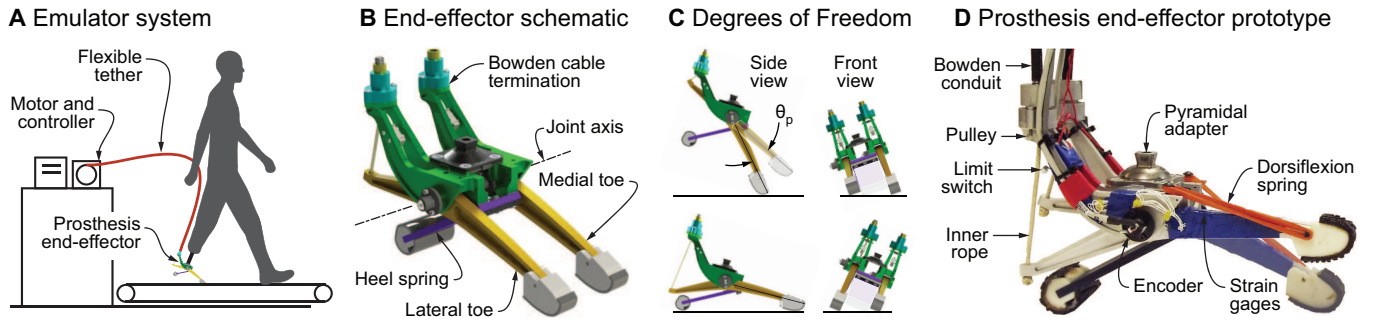


Fig. 1. Mechanical design of the two degree of freedom ankle-foot prosthesis emulator. **A** The emulator system consists of (1) powerful off-board actuation and control, (2) a flexible Bowden-cable tether, and (3) an instrumented end-effector worn by the user. **B** The prosthesis end-effector has two independently-actuated toes and a separate, passive heel spring. **C** Plantarflexion occurs when both toes move together and inversion-eversion occurs when the medial and lateral toes move in opposite directions. Plantarflexion and inversion-eversion torques are proportional to the sum and difference, respectively, of individual toe torques. **D** The prototype used in experiments is instrumented with encoders at each ankle joint and four strain gages in a Wheatstone bridge on each toe to measure torque. The device is connected to the user via a universal pyramidal adapter. Rubber bands dorsiflex toes during the swing phase of walking.

Torque control in robotic emulator systems can be improved with appropriate series elasticity. Adding a spring in series with a high-stiffness transmission can reduce sensitivity to unexpected actuator displacements [26] imposed by the human. Unfortunately, this compliance also reduces force bandwidth when the output is fixed, since the motor must displace further when stretching the spring. In a tethered system, the flexible transmission itself is likely to have significant compliance, which might provide sufficient series elasticity.

Here we describe the design and evaluation of a robotic ankle-foot prosthesis emulator system with active control of both plantarflexion and inversion-eversion torques. We designed an end-effector that allowed inversion-eversion using two articulated toes, which we aimed to make lightweight and strong. We integrated the end-effector with existing off-board motor and control hardware, expected to facilitate high-bandwidth torque control. The end-effector did not include explicit series elasticity, testing the sufficiency of axial compliance in the tether. We implemented a basic walking controller, intended to evaluate the system's potential for emulating prosthesis behavior during interactions with a human user. We expect this approach to result in validation of system that can explore new dimensions of prosthesis assistance, particularly those related to balance during walking.

## II. METHODS

We designed and constructed an ankle-foot prosthesis end-effector with torque control in both plantarflexion and inversion-eversion directions. We characterized system performance, including peak torque and torque tracking, during dynamic tasks both on the benchtop and during walking.

### A. Mechanical Design

The two degree of freedom ankle-foot prosthesis was designed as an end-effector for a tethered emulator system (Fig. 1A). Powerful actuation and control hardware are located off-board so as to keep worn mass low. Flexible Bowden-cable tethers transmit mechanical power to the prosthesis, but do not interfere with natural movements of the limb. The motor, real-time controller and tether are described in detail in [21].

The ankle-foot prosthesis achieves torque and motion in both plantarflexion and inversion-eversion directions using two independent toes. The toes share a single axis of rotation similar to the plantarflexion axis in the human ankle joint, and are spaced medial-laterally such that one is closer to the centerline of the body (Fig. 1B). Plantarflexion occurs when both toes rotate in the same direction, and inversion-eversion occurs when they rotate in opposite directions (Fig. 1C). We define plantarflexion angle as the average of the toe angles and inversion-eversion angle as the difference between toe angles multiplied by the ratio of toe length to half the foot width. Similarly, plantarflexion torque is defined as the sum of the toe torques, and inversion-eversion torque is defined as the difference between toe torques multiplied by the ratio of one half foot width to toe length. Toes are actuated through independent Bowden cable tethers and off-board motors, allowing independent control of medial and lateral toe torques.

Plantarflexion and inversion-eversion torques can be independently controlled, but maximum allowable inversion-eversion torque proportional to plantarflexion torque. When inversion-eversion torque is zero, the plantarflexion torque is divided evenly between the toes. As inversion torque increases towards its limit, the torque on the lateral toe approaches the total desired plantarflexion torque, while the torque on the medial toe approaches zero. When inversion (or eversion) torque equals plantarflexion torque divided by the ratio of toe length to half the foot width it cannot be increased further, since doing so would require negative torque on the medial (or lateral) toe. In other words, the maximum inversion-eversion torque is coupled to plantarflexion torque through toe ground reaction forces, which cannot become negative.

The prosthesis consists of a frame, two toes with revolute joints, and a compliant heel. The frame of the device (Fig. 1D) is connected to the user's pylon or socket via a universal pyramidal adapter. The frame houses needle roller bearings for toe joints, which have a double-shear construction. Each toe is long and thin, tapers towards its ends, and has an I-beam cross section, making it well-suited to three-point bending. One end of the toe contacts the ground, while the other end is acted on by the Bowden cable, with the hinge located in the middle.

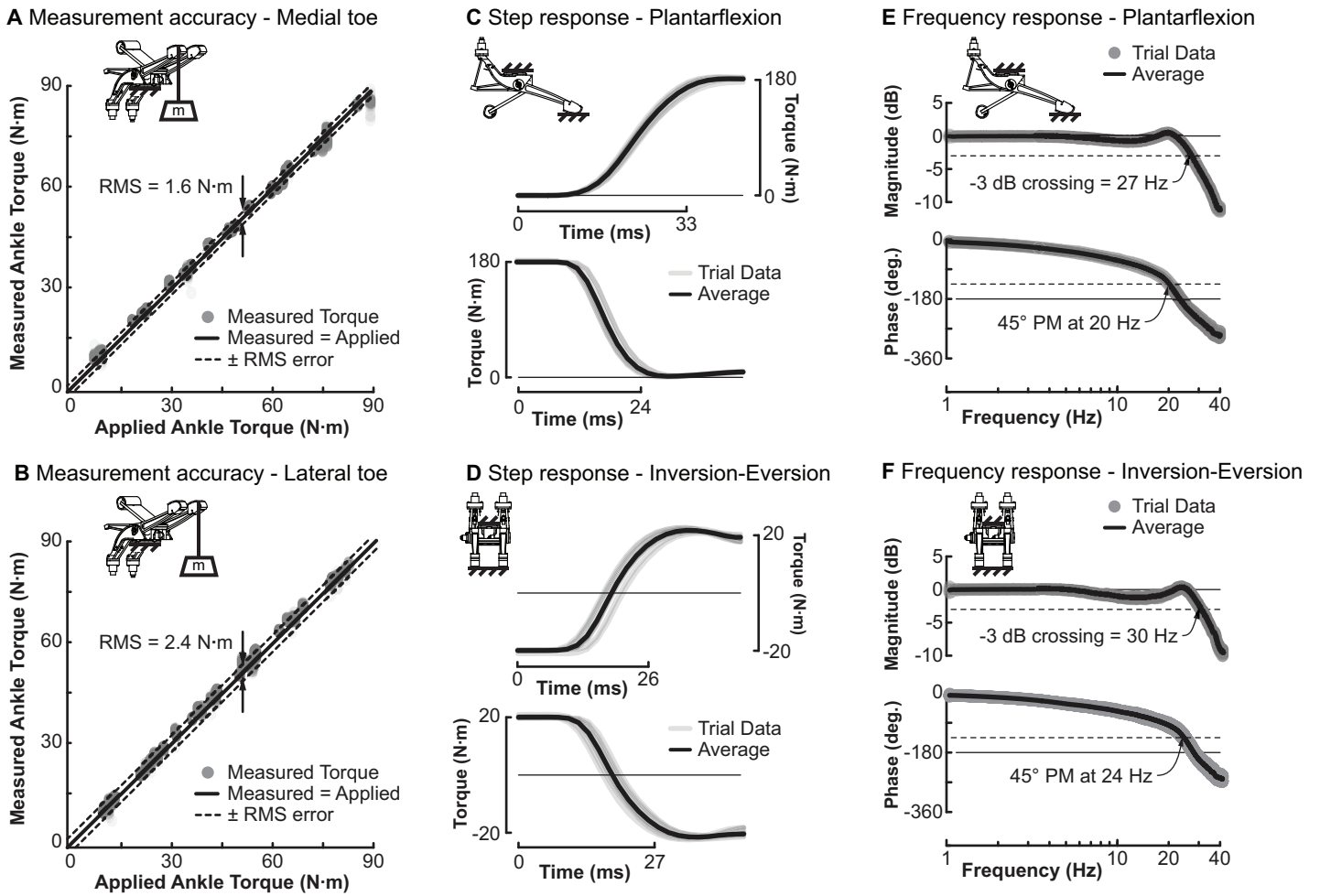


Fig. 2. Benchmark tests demonstrate low torque measurement error, high peak torque and high closed-loop torque bandwidth in both plantarflexion and inversion-eversion directions. Torque measurement validation for the **A** medial and **B** lateral toes. Step responses for closed-loop control of **C** plantarflexion and **D** inversion-eversion torque. Peak plantarflexion torque was at least 180 N·m, and inversion-eversion torque had a range of at least -20 to 20 N·m. Rise and fall times ranged from 0.024 to 0.033 s. Bode plots for closed-loop control of **E** plantarflexion and **F** inversion-eversion torque, calculated from responses to 90 N·m and  $\pm 20$  N·m magnitude chirps in desired torque, respectively. Bandwidth ranged from 20 to 30 Hz, limited by  $45^\circ$  phase margin.

When the inner rope of the Bowden cable pulls upwards on the posterior aspect of the toe, a moment is generated. The Bowden cable conduit presses down on the frame equally and oppositely, such that the foot experiences no net force from the transmission. Rubber bands act to dorsiflex the toe when the transmission allows, such as during the swing phase. A separate, unactuated heel spring is connected to the frame. Rubber-coated plastic pads are attached to the ends of the heel and toes for better ground contact. The frame and toes were machined from 7075-T6 aluminum, the heel spring was machined from fiberglass (GC-67-UB, Gordon Composites, Montrose, CO, USA), and the toe pads were fabricated using fused-deposition modeling of ABS plastic.

Prosthesis dimensions were based on those of the human foot [27]. The prosthesis measures 0.23 m in length, heel to toe, 0.07 m in width, toe center to toe center, and 0.08 m in height, from ground to ankle joint. The toe length, from axis of rotation to tip, is 0.14 m. Ankle range of motion is  $-20^\circ$  to  $30^\circ$  in plantarflexion and greater than  $-20^\circ$  to  $20^\circ$  in inversion-eversion. The prosthesis end-effector weighs 0.72 kg.

The end-effector did not include an explicit transmission spring, but some series elasticity was provided by the Bowden cable. Series elasticity can improve torque tracking in the presence of disturbances from the human user. In our prior designs [20, 28], we used fiberglass leaf springs or steel coil springs at the connection between the Bowden cable and the hinged foot element. In this design, we explored whether the compliance of the Bowden cable itself might be sufficient to facilitate low-error torque tracking. With increased series stiffness, we expected joint torque to change more quickly when toes were fixed and the motor was rotated, resulting in higher closed-loop torque bandwidth. However, we also expected torques to change more quickly when the motor was stationary and the toes were unexpectedly rotated, for example during initial contact with the ground, which could result in poorer torque tracking under realistic conditions.

Medial and lateral toe joint angles were sensed individually using digital absolute magnetic encoders (MAE3, US Digital, Vancouver, WA, USA). Toe torques were sensed using strain gages (SGD-3, Omega Engineering, Stamford, CT, USA),

configured in a Wheatstone bridge, with two gages on the top and bottom surfaces of each toe near the ankle joint. Bridge voltage was amplified (FSH01449, Futek, Irvine, CA, USA), sampled at a frequency of 5000 Hz and low-pass filtered with a cutoff frequency of 200 Hz. In an earlier revision of this design, Bowden cable tension was sensed using pushbutton load cells at the conduit termination (inside the cyan elements in Fig. 1B). This resulted in parasitic loads from the cable and hysteresis due to friction at the termination. Plantarflexion and inversion-eversion angles and torques were calculated in software from medial and lateral toe values.

### B. Control

We used a variation on classical feedback control to regulate torque during benchtop tests, with an additional iterative learning term during walking trials. Desired torque for each toe was first calculated from desired plantarflexion and inversion-eversion torques. Motor velocities were then commanded using proportional control on toe torque error and damping injection on measured motor velocity. Compliance between the off-board motor and prosthesis toes mean motor velocity is similar to the rate of change in toe torque. During walking trials, an additional time-based iterative learning term was added, which provided feed-forward compensation of torque errors that tended to occur at the same time each step. This method is described in detail in [24].

In walking trials, torque control was used during stance and position control was used during swing. Initial toe contact was sensed from an increase in toe torque upon making contact with the ground. During the ensuing stance period, desired inversion-eversion torque was set to a constant value, providing a simple demonstration of platform capabilities. Desired plantarflexion torque during stance was calculated as a function of plantarflexion angle [20] so as to approximate the torque-angle relationship observed during normal walking [29]. Toe off was detected when plantarflexion torque crossed a minimum threshold. During the ensuing swing phase, toes were position controlled to provide ground clearance.

### C. Experimental Methods

We conducted benchtop tests to characterize device performance in terms of torque measurement accuracy, response time, bandwidth, and disturbance rejection. We performed walking trials to assess mechatronic performance under similar conditions as expected during biomechanics experiments.

Torque measurement calibration was performed by applying known forces to the end of each toe using free weights and fitting amplified strain gage bridge voltage to applied torque. Measurement accuracy was characterized in a separate validation test as root mean squared (RMS) error between applied and measured toe torques.

Step response tests were performed in which we rigidly fixed the prosthesis frame and toes and commanded desired torque as a square wave from 0 to 180 N·m in plantarflexion or -20 to 20 N·m in inversion-eversion. We conducted 10 trials for

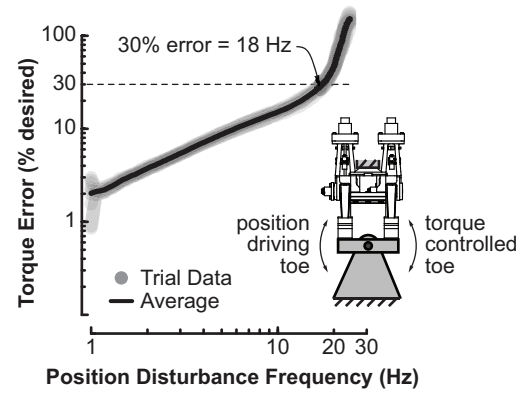


Fig. 3. Disturbance rejection, depicted as the relationship between torque error in % of the constant desired value versus the frequency of an applied disturbance in toe position. This characterizes the ability of the system to reject unexpected environmental disturbances, such as from sudden contact with the ground. Torque error was less than 30% of the desired value for disturbance frequencies up to 18 Hz.

each direction and computed the mean and standard deviation of the 90% rise and fall times.

We performed bandwidth tests in which desired torque was commanded as a 0 to 40 Hz chirp, oscillating between 10 and 90 N·m for plantarflexion and between -20 and 20 N·m for inversion-eversion. We used an exponential chirp to improve signal to noise ratio in the low frequency range. We transformed the desired and measured torque into the frequency domain using a Fast Fourier Transform and used the magnitude ratio and phase difference to generate a Bode plot. We calculated the gain-limited and phase-limited bandwidths [30] as the frequencies at which the amplitude ratio was -3 dB and the phase margin was 45°, respectively. We performed 10 trials for both torques and calculated crossover frequency means and standard deviations.

We also performed a test intended to evaluate the torque errors that would arise from unexpected disturbances to toe position. We expected that high series stiffness in this system might have provided high bandwidth at the cost of higher sensitivity to position disturbances, for example during initial toe contact with the ground. We placed the toes on opposite ends of a seesaw-like testing jig such that toe forces were equal and toe motions were equal and opposite. We then applied a 0 to 25 Hz chirp in medial toe position, oscillating between 0° and 5° of plantarflexion (or 0 and 0.012 m of toe tip displacement) and commanded a constant desired torque of 30 N·m to the lateral toe. We transformed the amplitude of the resulting torque error into the frequency domain using a Fast Fourier Transform, reported as a percent of the constant desired torque magnitude. We calculated the frequency at which error rose above 30% of the desired torque, analogous to the -3 dB (70% amplitude) criteria used in bandwidth tests.

We performed walking trials to evaluate torque tracking performance under realistic conditions. One subject (67 kg, 1.77 m tall, 23 yrs, male) without amputation wore the device using a simulator boot [31]. Five walking trials were conducted in which desired inversion-eversion torque,  $\tau_{inv}$ , was commanded as: Maximum, 15 N·m, 0 N·m, -15 N·m,

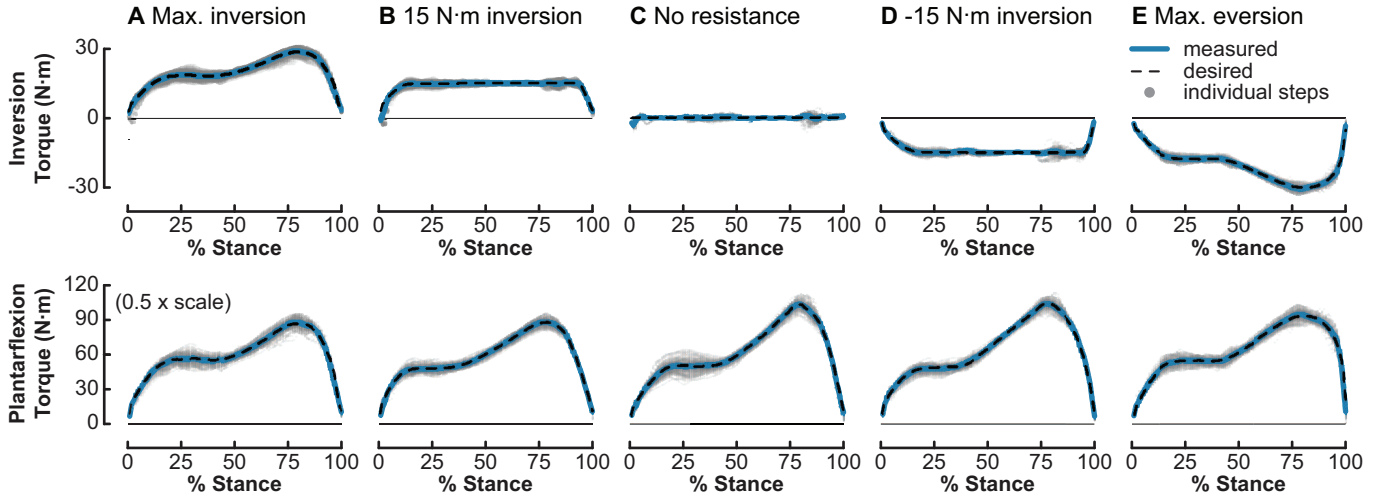


Fig. 4. Torque tracking during walking experiments. Desired ankle inversion torque set to **A** Maximum, **B** 15 N-m, **C** zero, **D** -15 N-m, and **E** Maximum Negative, while desired plantarflexion torque was a consistent function of ankle plantarflexion angle. Maximum and Maximum Negative allowable inversion torque were limited by desired plantarflexion torque, since the toe ground reaction force could not be negative. In each 100-stride trial, measured torque closely matched desired torque, with RMS errors of at most 3.7 N-m in plantarflexion and 1.1 N-m in inversion-eversion across conditions. Differences between average torque and torque from individual steps were dominated by natural variability in the subject’s gait pattern.

and Maximum Negative. The magnitudes of Maximum and Maximum Negative inversion-eversion torque were proportional to plantarflexion torque at each instant in time. The subject walked on a treadmill at  $1.25 \text{ m}\cdot\text{s}^{-1}$  for 100 strides in each condition. We normalized each step to percent stance period and calculated an average step for each condition. We characterized torque tracking error as both the RMS error across the entire trial and as the RMS error of the average step. We did not measure human biomechanical response, since this study was intended to evaluate performance of the robotic system and not the effects of a proposed intervention.

### III. RESULTS

Benchmark tests revealed low torque measurement error, high peak torque and high closed-loop torque bandwidth. The root mean squared (RMS) torque measurement error for medial and lateral toes were 1.64 N-m and 2.43 N-m, respectively, following calibration (Fig. 2A&B). The 90% rise and fall times between 0 and 180 N-m in plantarflexion torque were  $0.033 \pm 0.001 \text{ s}$  and  $0.024 \pm 0.001 \text{ s}$  (mean  $\pm$  s.d.), with 0.5% and 1.6% overshoot, respectively (Fig. 2C). The 90% rise and fall times between -20 to 20 N-m in inversion-eversion torque were  $0.026 \pm 0.002 \text{ s}$  and  $0.027 \pm 0.002 \text{ s}$ , with 3.0% and 3.2% overshoot, respectively (Fig. 2D). With desired plantarflexion torque oscillating between 10 and 90 N-m, the -3 dB magnitude and  $45^\circ$  phase margin crossover frequencies were  $27.2 \pm 0.2 \text{ Hz}$  and  $21.4 \pm 0.3 \text{ Hz}$ , respectively (Fig. 2E). With desired inversion-eversion torque oscillating between -20 and 20 N-m, the -3 dB magnitude and  $45^\circ$  phase margin crossover frequencies were  $27.2 \pm 0.2 \text{ Hz}$  and  $21.4 \pm 0.3 \text{ Hz}$ , respectively (Fig. 2F).

When we applied a 0.012 m amplitude chirp disturbance in toe endpoint position and commanded a constant desired torque of 30 N-m, torque error was less than 30% up to a disturbance frequency of 18 Hz (Fig. 3). This disturbance

frequency and amplitude are similar to unexpected contact with moderately compliant ground at a rate of  $44 \text{ m}\cdot\text{s}^{-1}$ .

In walking trials, the subject walked comfortably with the prosthesis while five levels of constant desired inversion-eversion torque were applied (Fig. 4). Torque tracking errors in both plantarflexion and inversion-eversion directions were low across all conditions, with maximum step-wise RMS errors of 3.2 N-m (3.7% of peak) and 1.6 N-m (3.8% of peak) in plantarflexion and inversion-eversion, respectively (Table I).

### IV. DISCUSSION

We designed, built and tested an ankle-foot prosthesis system with torque control in both plantarflexion and inversion-eversion directions. The end-effector was lightweight, having about 60% of the mass of a typical human foot [32] and about a third of the mass of other tethered [3, 14, 15] and untethered [2, 33] robotic ankle-foot prostheses. The device produced large torques in both plantarflexion and inversion-eversion directions, with peak measured plantarflexion and inversion-eversion torques that were 50% and 230% greater than observed during normal walking, respectively [19, 34], and similar to those in other devices with powered plantarflexion [2, 3, 33] or inversion-eversion [14]. The system had high closed-loop torque bandwidth, a limiting factor in the fidelity of haptic emulation [35]. Bandwidth was nearly twice that of our previous ankle-foot prosthesis platform [21], and about ten times that of similar systems using pneumatic muscles [3, 36]. Torque step response was about five times as fast as in a similar system with inversion-eversion torque produced by an on-board motor-driven linear actuator [14]. The prosthesis end-effector had low torque errors in the presence of unexpected toe displacements at high speeds, indicating robustness during unpredictable human interactions. During walking trials, a wide range of inversion-eversion torque values were tracked with low error. Taken as a whole, these results demonstrate

TABLE I  
TORQUE TRACKING ERRORS DURING 100 STEPS OF WALKING WITH VARIOUS VALUES OF DESIRED INVERSION-EVERSION TORQUE.

Inversion-eversion torque	Plantarflexion Torque Tracking				Inversion-Eversion Torque Tracking			
	RMS error	% $\tau_{max}$	AVG RMS error	% $\tau_{max}$	RMS error	% $\tau_{max}$	AVG RMS error	% $\tau_{max}$
$\tau_{inv} = \text{Maximum}$	$3.2 \pm 1.1$ N·m	3.7%	1.3 N·m	1.6%	$1.6 \pm 1.1$ N·m	3.8%	0.4 N·m	1.6%
$\tau_{inv} = -15$ N·m	$1.9 \pm 0.4$ N·m	2.2%	0.7 N·m	0.8%	$0.9 \pm 0.2$ N·m	5.9%	0.7 N·m	4.4%
$\tau_{inv} = 0$	$2.9 \pm 1.7$ N·m	2.8%	0.6 N·m	0.6%	$0.8 \pm 0.2$ N·m	-	0.5 N·m	-
$\tau_{inv} = -15$ N·m	$2.9 \pm 0.8$ N·m	2.8%	0.9 N·m	0.8%	$0.8 \pm 0.2$ N·m	5.6%	0.3 N·m	2.1%
$\tau_{inv} = \text{Negative Maximum}$	$3.0 \pm 0.9$ N·m	3.3%	1.3 N·m	1.4%	$1.0 \pm 0.3$ N·m	3.3%	0.4 N·m	1.6%

the versatility of the ankle-foot prosthesis emulator and its suitability for haptic emulation of prostheses with both pitch and roll degrees of freedom.

Although this design does not include an explicit series spring in the end-effector, disturbance rejection was relatively high and torque tracking errors were low during walking. It appears that series elasticity provided by stretch in the Bowden cable transmission sufficiently decoupled the toes from the inertia of the motor. This has not been the case for all emulator end-effectors we have tested. In pilot tests with an ankle exoskeleton [24], we found that removing the coil spring at the ankle joint greatly increased torque tracking errors. Differences may be related to the types of disturbance provided by the human in these cases; having muscles in parallel with the actuator, as with an exoskeleton, may produce larger or higher-frequency variations in interaction torques than when a prosthesis is placed in series with the limb. In this system, torque measurement was also not adversely affected by lack of a series spring. Measuring torque using spring deflection [20, 37] can reduce electromagnetic noise compared to strain gages [26]. In this case, the amplified strain gage bridge voltage exhibited noise in the kHz range, but this was easily removed by sampling at high frequency and low-pass filtering.

Using two toes for inversion-eversion results in a simple, lightweight structure, but does not provide direct measurement of frontal-plane motions. The angle of the shank with respect to vertical in the frontal plane cannot be calculated from the angles of the medial and lateral toes alone (unless they are equal), since rotation about the line between toe contact points is not captured by joint angles. More sensory information, such as the pitch angle of the prosthesis frame, is required. A similar problem arises if inversion-eversion torque is defined about an axis in the direction of travel. In a laboratory setting, this issue can be overcome by measuring shank angle directly with motion capture equipment. Another solution, which would also be suitable for autonomous devices, would be to (actively) maintain heel contact throughout stance, thereby obtaining the missing configuration-related measurement.

The prosthesis emulator has high-fidelity control over the medial-lateral location of the center of pressure during stance, but would require an additional active degree of freedom to usefully control fore-aft center of pressure location. Humans seem to regulate the path of the center of pressure during walking [38], making this a potentially interesting signal for manipulation. In this system, the medial-lateral center of pressure can be controlled through inversion-eversion torque when both toes contact the ground. In the fore-aft direction,

the center of pressure can only be controlled when the heel is also in contact. Since the heel is passive, contact is maintained only for a limited range of shank and toe configurations. Active torque control of the heel would resolve this issue.

Although we have not yet tested this system on subjects with amputation, we expect similar haptic emulation performance under such conditions. Human response to robotic intervention can depend strongly upon subject characteristics [39], but device behavior typically does not. Benchtop measurements are, of course, subject-independent. This study concerned the mechatronic performance of the prosthesis emulator, whereas future studies probing biomechanical response to different interventions will require multiple subjects with amputation.

## V. CONCLUSIONS

We have described the design of a tethered ankle-foot prosthesis emulator system with independent control over plantarflexion and inversion-eversion torque. Benchtop tests and experiments during human walking provided a detailed characterization of system dynamics and performance, which we expect will guide the design of improved systems. The torque control fidelity of this platform was exceptional, particularly in terms of closed-loop torque bandwidth, making it suitable for haptic emulation of prostheses with pitch and roll degrees of freedom. A wide variety of virtual devices could be rendered to users as part of the clinical prescription process [23], during the development of new commercial devices [22], or in basic science experiments probing the nature of human locomotion [31]. In particular, we expect experiments with this system to provide insights into the role of inversion-eversion torque on walking balance for individuals with amputation.

## VI. ACKNOWLEDGMENTS

The authors thank Josh Caputo, Zach Batts, Winton Zheng, Tanuf Tembulkar and Tyler del Sesto for their contributions to the development of system hardware and software.

- [1] F. Sup *et al.*, "Self-contained powered knee and ankle prosthesis: Initial evaluation on a transfemoral amputee," in *Proc. Int. Conf. Rehab. Rob.*, 2009, pp. 638–644.
- [2] H. M. Herr and A. M. Grabowski, "Bionic ankle-foot prosthesis normalizes walking gait for persons with leg amputation," *Proc. Roy. Soc. Lon. B*, vol. 279, pp. 457–464, 2012.
- [3] S. Huang, J. P. Wensman, and D. P. Ferris, "An experimental powered lower limb prosthesis using proportional myoelectric control," *J. Med. Dev.*, vol. 8, p. 024501, 2014.
- [4] A. M. Dollar and H. Herr, "Lower extremity exoskeletons and active orthoses: challenges and state-of-the-art," vol. 24, pp. 144–158, 2008.
- [5] M. Goldfarb, B. E. Lawson, and A. H. Schultz, "Realizing the promise of robotic leg prostheses," *Sci. Trans. Med.*, vol. 5, pp. 1–6, 2013.

- [6] College Park, "College Park - Trustep," September, 2014. URL: <http://www.college-park.com/prosthetics/trustep>.
- [7] Össur, "Vari-Flex."
- [8] A. L. Hof *et al.*, "Control of lateral balance in walking: Experimental findings in normal subjects and above-knee amputees," *Gait Post.*, vol. 25, pp. 250–258, 2007.
- [9] A. D. Kuo, "Stabilization of lateral motion in passive dynamic walking," *Int. J. Rob. Res.*, vol. 18, pp. 917–930, 1999.
- [10] S. M. Bruijn *et al.*, "The effects of arm swing on human gait stability," *J. Exp. Biol.*, vol. 213, pp. 3945–3952, 2010.
- [11] T. Ijmker *et al.*, "Can external lateral stabilization reduce the energy cost of walking in persons with a lower limb amputation?" vol. 40, pp. 616–621, 2014.
- [12] D. H. Gates *et al.*, "Frontal plane dynamic margins of stability in individuals with and without transtibial amputation walking on a loose rock surface," vol. 38, pp. 570–575, 2013.
- [13] W. C. Miller *et al.*, "The influence of falling, fear of falling and balance confidence on prosthetic mobility and social activity among individuals with a lower extremity amputation," *Arch. Phys. Med. Rehab.*, vol. 82, pp. 1238–1244, 2001.
- [14] J. T. Panzenbeck and G. K. Klute, "A powered inverting and everting prosthetic foot for balance assistance in lower limb amputees," vol. 24, pp. 175–180, 2012.
- [15] E. M. Ficanha *et al.*, "Ankle angles during step turn and straight walk: Implications for the design of a steerable ankle-foot prosthetic robot," in *Proc. DSCC*, 2013, pp. 1–5.
- [16] R. D. Bellman, M. A. Holgate, and T. G. Sugar, "SPARKy 3: Design of an active robotic ankle prosthesis with two actuated degrees of freedom using regenerative kinetics," in *Proc. BioRob*, 2008, pp. 511–516.
- [17] A. Roy *et al.*, "Robot-aided neurorehabilitation: a novel robot for ankle rehabilitation," *Trans. Rob.*, vol. 25, pp. 569–582, 2009.
- [18] J. J. Eng and D. A. Winter, "Kinetic analysis of the lower limbs during walking: what information can be gained from a three-dimensional model?"
- [19] A. E. Hunt, R. M. Smith, and M. Torode, "Extrinsic muscle activity, foot motion and ankle joint moments during the stance phase of walking," *Foot & Ankle*, vol. 22, pp. 31–41, 2001.
- [20] J. M. Caputo and S. H. Collins, "An experimental robotic testbed for accelerated development of ankle prostheses," in *Proc. Int. Conf. Rob. Autom.*, 2013, pp. 2630–2635.
- [21] —, "A universal ankle-foot prosthesis emulator for experiments during human locomotion," *J. Biomech. Eng.*, vol. 136, p. 035002, 2014.
- [22] S. H. Collins, "What do walking humans want from mechatronics? (invited presentation)," in *Int. Conf. Mech.*, 2013.
- [23] S. H. Collins, J. M. Caputo, and P. G. Adamczyk, "Emulating prosthetic feet during the prescription process to improve outcomes and justifications," in *Proc. ARSO*, 2014, pp. 1–2.
- [24] J. Zhang, C. Cheah, and S. H. Collins, "A systematic comparison of nine prominent torque control methods in a tethered ankle exoskeleton with series elastic actuation during human walking," *Int. J. Rob. Res.*, vol. submitted, 2014.
- [25] M. Kim and S. H. Collins, "Once-per-step control of ankle-foot prosthesis push-off work reduces effort associated with balance during walking," *J. Roy. Soc. Int.*, vol. submitted, 2014.
- [26] G. Pratt and M. Williamson, "Series elastic actuators," in *Proc. Int. Conf. Intel. Rob. Sys.*, 1995.
- [27] M. R. Hawes and D. Sovak, "Quantitative morphology of the human foot in a North American population," *Ergonomics*, vol. 37, pp. 1213–1226, 1994.
- [28] K. A. Witte, J. Zhang, and R. W. Jackson, "Design of two lightweight torque-controlled ankle exoskeletons," in *Proc. Int. Conf. Rob. Autom.*, 2015, p. submitted.
- [29] D. A. Winter, *The Biomechanics and Motor Control of Human Gait: Normal, Elderly and Pathological*. Waterloo, Canada: Waterloo Biomechanics, 1991.
- [30] K. Warwick, *An Introduction to Control Systems*, 2nd ed. Singapore: World Scientific, 1996.
- [31] J. M. Caputo and S. H. Collins, "Prosthetic ankle push-off work reduces metabolic rate but not collision work in non-amputee walking," *Sci. Rep.*, vol. submitted, 2014.
- [32] D. A. Winter, *Biomechanics and Motor Control of Human Movement*, 2nd ed. Toronto, Canada: John Wiley & Sons, Inc., 1990.
- [33] A. H. Shultz *et al.*, "Preliminary evaluation of a walking controller for a powered ankle prosthesis," in *Proc. Int. Conf. Rob. Autom.*, 2013, pp. 4823–4828.
- [34] M. Whittle, *Gait Analysis: An Introduction*. Oxford, United Kingdom: Butterworth-Heinemann, 1996.
- [35] P. G. Griffiths, R. B. Gillespie, and J. S. Freudenberg, "A fundamental linear systems conflict between performance and passivity in haptic rendering," *Trans. Rob.*, vol. 27, pp. 75–88, 2011.
- [36] K. E. Gordon, G. S. Sawicki, and D. P. Ferris, "Mechanical performance of artificial pneumatic muscles to power an ankle-foot orthosis," *J. Biomech.*, vol. 39, pp. 1832–1841, 2006.
- [37] J. Pratt, B. Krupp, and C. Morse, "Series elastic actuators for high fidelity force control," *Indust. Rob: Int. J.*, vol. 29, pp. 234–241, 2002.
- [38] A. H. Hansen, D. S. Childress, and E. H. Knox, "Roll-over shapes of human locomotor systems: effects of walking speed," vol. 19, 2004.
- [39] K. E. Zelik *et al.*, "Systematic variation of prosthetic foot parameter affects center-of-mass mechanics and metabolic cost during walking," *Trans. Neural Syst. Rehabil. Eng.*, vol. 19, pp. 411–419, 2011.